



ELSEVIER

Available online at [www.sciencedirect.com](http://www.sciencedirect.com)

SCIENCE @ DIRECT®

Earth and Planetary Science Letters 216 (2003) 467–481

EPSL

[www.elsevier.com/locate/epsl](http://www.elsevier.com/locate/epsl)

# Zirconium isotope evidence for incomplete admixing of *r*-process components in the solar nebula

Maria Schönbächler<sup>a,\*</sup>, Der-Chuen Lee<sup>a</sup>, Mark Rehkämper<sup>a</sup>,  
Alex N. Halliday<sup>a</sup>, Manuela A. Fehr<sup>a</sup>, Bodo Hattendorf<sup>b</sup>, Detlef Günther<sup>b</sup>

<sup>a</sup> *ETH Zürich, Institute of Isotope Geology and Mineral Resources, 8092 Zürich, Switzerland*

<sup>b</sup> *ETH Zürich, Laboratory of Inorganic Chemistry, 8093 Zürich, Switzerland*

Received 30 March 2003; received in revised form 14 July 2003; accepted 14 September 2003

## Abstract

Isotopic anomalies in Mo and Zr have recently been reported for bulk chondrites and iron meteorites and have been interpreted in terms of a primordial nucleosynthetic heterogeneity in the solar nebula. We report precise Zr isotopic measurements of carbonaceous, ordinary and enstatite chondrites, eucrites, mesosiderites and lunar rocks. All bulk rock samples yield isotopic compositions that are identical to the terrestrial standard within the analytical uncertainty. No anomalies in <sup>92</sup>Zr are found in any samples including high Nb/Zr eucrites and high and low Nb/Zr calcium–aluminum-rich inclusions (CAIs). These data are consistent with the most recent estimates of  $< 10^{-4}$  for the initial <sup>92</sup>Nb/<sup>93</sup>Nb of the solar system. There exists a trace of isotopic heterogeneity in the form of a small excess of *r*-process <sup>96</sup>Zr in some refractory CAIs and some metal-rich phases of Renazzo. A more striking enrichment in <sup>96</sup>Zr is found in acetic acid leachates of the Allende CV carbonaceous chondrite. These data indicate that the *r*- and *s*-process Zr components found in presolar grains were well mixed on a large scale prior to planetary accretion. However, some CAIs formed before mixing was complete, such that they were able to sample a population of *r*-process-enriched material. The maximum amount of additional *r*-process component that was added to the otherwise well-mixed Zr in the molecular cloud or disk corresponds to  $\sim 0.01\%$ .

© 2003 Elsevier B.V. All rights reserved.

*Keywords:* cosmochemistry; isotopes; radioactivity; planetary sciences; meteorites

## 1. Introduction

The isotopic homogeneity of the early solar nebula is a central issue of cosmochemistry. Until

the early 1970s, the isotopic compositions of a range of elements in meteorites had been found to be identical, within uncertainties, to those in the Earth. For example, no significant variation could be found in the isotope abundances of K, Rb and Sr in chondrites, eucrites and the Earth, once the effects of mass-dependent fractionation, cosmic ray-induced spallation and radioactive decay were removed [1]. This large-scale homogeneity led to the view that the protoplanetary disk

\* Corresponding author. Tel.: +41-1-632-47-30;

Fax: +41-1-632-18-27.

E-mail address: [maria@erdw.ethz.ch](mailto:maria@erdw.ethz.ch) (M. Schönbächler).

was made of material that condensed from a hot well-mixed nebular gas.

This paradigm gradually changed, however, with the detection of small-scale isotopic anomalies in chondrites. Previously unknown isotopic effects in oxygen were discovered in refractory calcium–aluminum-rich inclusions (CAIs) [2]. Subsequently, further isotopic heterogeneities in CAIs were found for a variety of elements such as titanium [3], samarium [4], neodymium and barium [5]. The discovery of presolar grains [6] and dispersed  $^{54}\text{Cr}$  isotopic anomalies in Orgueil [7] provided strong evidence that the disk also contained presolar material that had not condensed from a hot nebular gas.

With small-scale heterogeneity in chondrites now well established, one has to re-examine the question of what large-scale homogeneity signifies if it is not produced in a well-mixed gas. Two extreme models can be considered:

1. The various presolar components were already well mixed in the molecular cloud before the collapse of the solar nebula.
2. There were processes in the disk that averaged out heterogeneity. The early dynamics of disks are thought to be dominated by settling of dust onto the mid-plane, the swirling motion of the nebula, the rapid accretion of planetesimals and the overall migration of material in toward the sun [8]. Some have proposed that material may also have been transported outwards from the sun across the disk [9]. It is conceivable that disks develop into conveyor belts prior to the creation of major gaps that are formed by incorporating gas and dust into large planetary objects. This swirling ‘conveyor belt’ might be the most likely environment for mixing [8].

Although the evidence for large-scale homogeneity in the disk is overwhelming, there also exist indications of large-scale heterogeneity. The first clear evidence followed the realization that basaltic achondrites such as angrites, eucrites and Martian meteorites possess distinctive oxygen isotopic compositions that are characteristic of their parent bodies and different from those of the Earth and Moon [10]. It has now become well established that the solar system possesses a large-scale

heterogeneity in oxygen isotopes. The heterogeneity in  $\Delta^{17}\text{O}$  is not a function of heliocentric distance and may be caused by varying degrees of exchange between a gas and a solid reservoir [11]. Why gases and solids should have had different oxygen isotope compositions is unclear.

Evidence for large-scale isotopic heterogeneity that cannot be explained by gas–solid mixing is far more equivocal, however. From the discovery of small  $^{53}\text{Cr}$  abundance variations, which are a function of heliocentric distance, a former radial zonation in  $^{53}\text{Mn}$  in the inner solar system has been proposed [12]. Alternatively, this observation can also be explained by volatility-induced Mn/Cr fractionation, with the exception of the  $^{53}\text{Cr}$  abundances in enstatite chondrites (EH) [13–15]. Recently, it has been proposed that there are small molybdenum isotopic variations in bulk rock chondrites and iron meteorites [16,17]. However, other studies based on more extensive replication and/or higher precision indicate that these effects are not yet well-defined [18,19].

The best way to approach this issue is with high-precision measurements of the relative abundances of isotopes produced via different nucleosynthetic pathways. A constant proportion of isotopes produced in different stellar environments would indicate very efficient mixing of components at some early or presolar stage. Small variations in the relative abundances have implications for how components must have been introduced and admixed into the solar nebula.

Zirconium is a promising element to address the question of isotopic homogeneity in the inner solar system. It is refractory and, therefore, insensitive to early solar system processes controlled by volatility that may influence elements like Mn, and hence Mn–Cr systematics. All Zr isotopes have mixed nucleosynthetic sources, but are dominated by one process.  $^{96}\text{Zr}$  is primarily produced by the *r*-process, whereas all the other Zr isotopes ( $^{90}\text{Zr}$ ,  $^{91}\text{Zr}$ ,  $^{92}\text{Zr}$ ,  $^{94}\text{Zr}$ ) predominantly originate from the *s*-process. Excess  $^{96}\text{Zr}$  relative to the other Zr isotopes and the terrestrial standard was reported for presolar grains [20,21], and explained as due to *r*-process material produced in supernovae [22]. It may also be that some of the  $^{96}\text{Zr}$  was made by the *s*-process if the neutron

density was unusually high [20]. However, this is speculative at this stage. A complementary pattern with a deficit of  $^{96}\text{Zr}$  was found in presolar grains [23]. Such grains display an overabundance of *s*-process nuclides, which may have formed in AGB stars [22]. Moreover, two independent studies have claimed that there are well-resolved bulk rock isotopic variations of zirconium in chondrites [24,25], and these were interpreted to reflect incomplete mixing of different nucleosynthetic components. In particular, Yin et al. [25] reported a very large  $^{96}\text{Zr}$  anomaly for the carbonaceous chondrite Murchison.

The isotope  $^{92}\text{Zr}$  is also produced by the radioactive decay of the short-lived radionuclide  $^{92}\text{Nb}$  ( $t_{1/2} = 36 \pm 3$  Myr) [26]. For the application of this short-lived isotopic system, it is crucial to know if Nb and Zr isotopes are distributed homogeneously in the solar system. The initial abundance of  $^{92}\text{Nb}$  has been a matter of recent debate. Current estimates range from an initial  $^{92}\text{Nb}/^{93}\text{Nb}$  ratio of  $10^{-5}$  up to a value as high as  $10^{-3}$  [24,27–31].

The aim of this study was to investigate if Zr isotopes are indeed distributed heterogeneously in the inner solar system. For this purpose, a comprehensive Zr isotopic study was conducted on a wide range of samples, including CAIs, chondrites, differentiated meteorites, lunar and terres-

trial samples. The results provide new constraints on the maximum amount of incompletely admixed Zr from hypothetical triggering stars and on the initial abundance of  $^{92}\text{Nb}$  in the solar system.

## 2. Analytical procedure

The samples were crushed in a boron carbide or an aluminum oxide mortar under a laminar flow of filtered air to avoid contamination. Subsequently, a Parr<sup>®</sup> acid digestion bomb was used to ensure the complete dissolution of the samples, including any zircons. The mineral separates and leachates of Allende and Renazzo were obtained as outlined in Table 1. We started with 2 g of Allende, which was treated sequentially with a series of progressively stronger reagents. After each treatment, the sample was centrifuged and the supernatant was removed by pipette. Renazzo was first separated mechanically with a hand magnet (Table 1) to obtain a magnetic and a non-magnetic fraction. A second magnetic separation was performed for the magnetic fraction only. The non-magnetic residue of the second step was then combined with the bulk rock sample to form the metal-rich whole rock sample. The

Table 1  
Experimental procedure for the separates of Allende and Renazzo

Allende			
Step	Reagent	Procedure	Percent <sup>a</sup> total Zr
1	50% HAc	2 days, RT	6
2	4 M HNO <sub>3</sub>	5 days, RT	0.1
3	6 M HCl	1 day, 80°C	21
4	13.5 M HF+3 M HCl	4 days, 100°C	66
5	Aqua regia	3 h, 220°C, high pressure asher	7
Renazzo			
Fraction		Mechanical separation	Chemical separation
n.m.	non-magnetic fraction	metal removed with a hand magnet	
m.l.	magnetic leachate fraction	metal cleaned up twice with a hand magnet	6 M HCl+0.01 M HF, 5 min, 40°C
m.r. w.r.	metal-rich whole rock	whole rock+metal-rich residue of second clean-up of the magnetic fraction	

RT = room temperature.

HAc = CH<sub>3</sub>COOH.

<sup>a</sup> Percentage of total recovered Zr dissolved in this fraction.

magnetic fraction was subsequently leached for 5 min with 6 M HCl–0.01 M HF to produce a magnetic leachate. The residue was too small for further treatment.

Zirconium was chemically separated from the whole rock matrix using a two-stage ion exchange procedure. The first and the second stage are adapted from Salters et al. [32] and Barovich et al. [33], respectively. The details will be discussed elsewhere [34]. The ion exchange procedure for the Allende leachates did not use hydrofluoric acid for the elution of Zr and an additional elution step for matrix elements with 15 M HF was included, such that we could also obtain a clean Te fraction. The Te data will be presented in a separate paper [35]. The modifications reduced the Zr yield to only about 30% in each sample. Such a low yield could potentially induce mass-dependent fractionation of Zr isotopes during chemistry. However, no such mass-dependent fractionation has been observed. The total chemistry blank for the Allende leachates was less than 3 ng Zr. This is negligible, considering that each sample fraction contained more than 300 ng Zr. The total chemistry blank for all other samples was always less than 1 ng Zr.

The Zr isotopic measurements were performed with a Nu Plasma multiple collector inductively coupled plasma mass spectrometer (ICP-MS) at the ETH Zürich. All Zr isotopes were measured, as well as  $^{95}\text{Mo}$ ,  $^{93}\text{Nb}$  and  $^{99}\text{Ru}$  in order to monitor potential isobaric interferences and peak-tailing effects. Instrumental mass fractionation was internally normalized to  $^{94}\text{Zr}/^{90}\text{Zr} = 0.3381$  [36] using the exponential law.  $\epsilon_{\text{Zr}}$  values were calculated relative to the mean values of the NIST SRM 3169 Zr standard solution measured the same day using  $\epsilon^{9x}\text{Zr} = \{[(^{9x}\text{Zr}/^{90}\text{Zr})_{\text{meas}} - (^{9x}\text{Zr}/^{90}\text{Zr})_{\text{std}}] / (^{9x}\text{Zr}/^{90}\text{Zr})_{\text{std}}\} \times 10^4$ . The  $2\sigma$  reproducibility obtained for 100 ppb solutions of the NIST SRM 3169 Zr standard is better than  $\pm 0.3$ ,  $\pm 0.6$  and  $\pm 1.2$   $\epsilon$  units for  $^{92}\text{Zr}$ ,  $^{91}\text{Zr}$  and  $^{96}\text{Zr}$ , respectively, within 1 day. We use these values as a conservative estimate of the analytical uncertainty for our standard solution. The long-term reproducibility is only slightly larger than the within-day precision [37].

The  $^{91}\text{Zr}$  analysis is hampered by a minor un-

identified interference, which is common to all samples and standards analyzed at low ion beams (total ion beam  $< 2.5 \times 10^{-11}$  A). The effect disappears at higher ion beams. It was compensated by measuring standards and samples with the same beam intensities [34]. However, most samples achieved total ion beams of  $\geq 5 \times 10^{-11}$  A. The Mo interference on mass 92 can be adequately corrected, if Mo/Zr in the sample solution is  $< 0.01$ , as inferred from repeated measurements of synthetic Mo–Zr mixtures. For an adequate correction of the  $^{96}\text{Mo}$  interference an even smaller Mo/Zr ratio of  $< 0.005$  is required, and a Ru/Zr ratio of  $< 0.01$  is necessary to adequately correct for the  $^{96}\text{Ru}$  interference. These limits correspond to a relative magnitude of the Mo and Ru corrections in the order of 1–3%. The Mo/Zr and Ru/Zr ratios of the analyzed sample solutions were always far below these limits. The Ru correction is essential for undifferentiated meteorites because they generally possess high Ru contents compared to the differentiated stony meteorites, lunar and terrestrial samples. For all differentiated samples, the Ru contribution to mass 96 was negligible and did not require correction. All samples were also carefully checked for interferences from Ti-, V-, Cr- and Fe-argides, which overlap with the masses of zirconium.

The  $^{93}\text{Nb}/^{90}\text{Zr}$  ratios of the samples were measured with a quadrupole ICP-MS on sample solution aliquots that did not undergo chemical separation, to avoid any chemical fractionation of Nb from Zr. Spectral interferences in these measurements were accounted for by using dynamic reaction cell technology with hydrogen as reactive gas [38].

### 3. Results

The Zr isotopic compositions ( $\epsilon^{91}\text{Zr}$ ,  $\epsilon^{92}\text{Zr}$ ,  $\epsilon^{96}\text{Zr}$ ) for bulk samples of four carbonaceous, eight ordinary and three enstatite chondrites are shown in Fig. 1a together with data for eucrites, a mesosiderite silicate clast and three lunar samples. Fig. 1a displays clearly that *all* bulk rock data are identical to the terrestrial standard within the  $2\sigma$  analytical uncertainty. Thus, there is

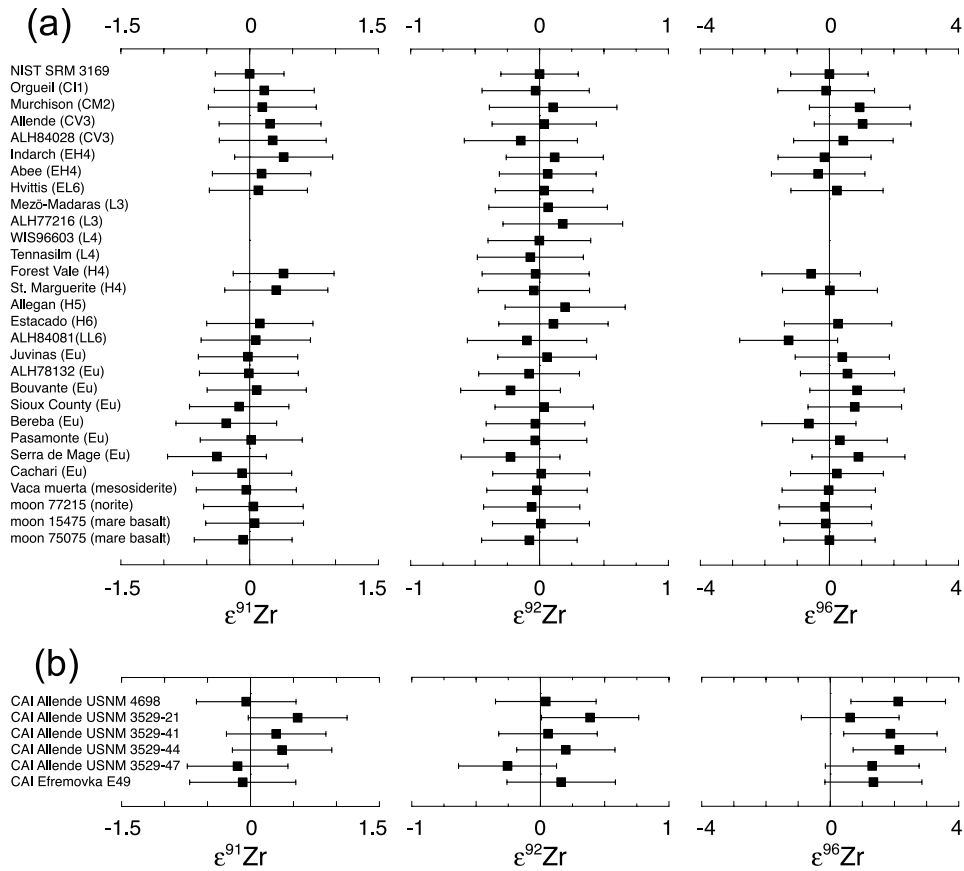


Fig. 1. (a) Zirconium isotopic compositions for various bulk meteorite samples. (b) Zirconium isotopic compositions for CAIs of Allende and Efremovka. Errors ( $2\sigma$ ) given for the samples include the external reproducibility of the sample and the standard combined as follows:  $\sigma^2 = \sigma_{\text{std}}^2 + \sigma_{\text{sam}}^2$ , where  $\sigma$  is the external reproducibility of the standard (std) or the sample (sam). If several analyses of a single sample exist (Table 2), the mean value is plotted. No  $\epsilon^{91}\text{Zr}$  and  $\epsilon^{96}\text{Zr}$  values are shown for some samples because of known interference problems and/or low signal intensities for the minor  $^{96}\text{Zr}$ . Eu = eucrite.

a striking homogeneity of Zr isotopic compositions.

Once the current analytical precision is improved it is possible that carbonaceous chondrites such as Murchison and Allende may reveal a slight shift to positive  $\epsilon^{96}\text{Zr}$  values. At present, this is not clearly resolvable. The repeated analyses of different Murchison and Allende aliquots (Table 2), however, show a small and systematic shift in  $\epsilon^{96}\text{Zr}$ . Furthermore, the application of a statistical  $t$ -test to compare the Murchison and Allende data sets with the terrestrial standard yields an explicit difference at the 99% confidence level. If this effect is not an analytical artefact, it indicates that Murchison and Allende have a

slightly different Zr isotopic composition than the Earth or that small-scale heterogeneities may exist within each sample. In summary, the primary conclusion is that bulk meteorite samples display identical Zr isotopic composition within the analytical uncertainty. Some results for carbonaceous chondrites hint at very small differences in  $\epsilon^{96}\text{Zr}$ , but the differences cannot be resolved unambiguously at present.

In contrast to the bulk rock data, two Allende leachates (acetic and hydrochloric acid steps) and three Renazzo fractions reveal evidence of significant excess  $^{96}\text{Zr}$  (Fig. 2). Interestingly, the results for Allende show that the Zr leached by the acetic acid displays the largest excess in  $^{96}\text{Zr}$

Table 2  
Zr isotopic data and Nb/Zr ratios

Sample	$\epsilon^{91}\text{Zr} \pm 2\sigma_{\text{mean}}$	$\epsilon^{92}\text{Zr} \pm 2\sigma_{\text{mean}}$	$\epsilon^{96}\text{Zr} \pm 2\sigma_{\text{mean}}$	Nb/Zr $\pm 2\sigma_{\text{mean}}$
Orgueil (CI1)	0.2 ± 0.6	0.0 ± 0.4	−0.1 ± 1.5	0.085 ± 0.004
Murchison (CM2)		0.2 ± 0.7		0.063 ± 0.003
Murchison (CM2)	0.1 ± 0.6	0.0 ± 0.4	1.2 ± 1.6	0.076 ± 0.004
Murchison (CM2)	0.1 ± 0.6	−0.1 ± 0.4	1.2 ± 1.6	0.072 ± 0.004
Murchison (CM2)	0.3 ± 0.6	0.3 ± 0.4	0.4 ± 1.5	0.063 ± 0.003
Allende (CV3)	0.5 ± 0.6	0.2 ± 0.4	1.2 ± 1.4	0.074 ± 0.005
Allende (CV3)	0.2 ± 0.6	−0.1 ± 0.4	0.9 ± 1.5	0.077 ± 0.004
Allende (CV3)	0.0 ± 0.6	0.0 ± 0.4	1.1 ± 1.4	0.074 ± 0.003
Allende (CV3)	0.5 ± 0.6	0.1 ± 0.5	0.7 ± 1.6	
Allende (CV3)	0.1 ± 0.6	−0.1 ± 0.4		
1.3{{decimal:split}} ± 1.5				
ALH84028 (CV3)	0.3 ± 0.6	−0.1 ± 0.4	0.4 ± 1.5	0.071 ± 0.006
Indarch (EH4)	0.4 ± 0.6	0.1 ± 0.4	−0.1 ± 1.4	
Abee (EH4)	0.1 ± 0.6	0.1 ± 0.4	−0.3 ± 1.4	
Hvittis (EL6)	0.1 ± 0.6	0.0 ± 0.4	0.2 ± 1.4	
Mező-Madaras (L3)		0.1 ± 0.5		0.076 ± 0.004
ALH77216 (L3)		0.2 ± 0.5		0.079 ± 0.004
WIS96603 (L4)		0.0 ± 0.4		0.085 ± 0.004
WIS96603 (L4)		0.0 ± 0.4		
Tennasilm (L4)		−0.1 ± 0.4		0.075 ± 0.004
Forest Vale (H4)	0.4 ± 0.6	0.0 ± 0.4	−0.6 ± 1.5	0.087 ± 0.008
St. Marguerite (H4)		−0.2 ± 0.5		0.081 ± 0.005
St. Marguerite (H4)	0.1 ± 0.6	0.1 ± 0.4	0.4 ± 1.4	
St. Marguerite (H4)	0.5 ± 0.6	0.0 ± 0.4	−0.4 ± 1.5	
Allegan (H5)		0.2 ± 0.5		0.078 ± 0.004
Estacado (H6)	0.1 ± 0.6	0.1 ± 0.4	0.3 ± 1.7	0.079 ± 0.004
ALH84081(LL6)	0.1 ± 0.6	−0.1 ± 0.5	−1.3 ± 1.5	0.070 ± 0.007
Juvinas (Eu)	0.0 ± 0.6	−0.2 ± 0.4	1.1 ± 1.4	0.098 ± 0.005
Juvinas (Eu)	−0.1 ± 0.6	0.3 ± 0.4	−0.3 ± 1.5	
ALH78132 (Eu)	0.0 ± 0.6	−0.1 ± 0.4	0.6 ± 1.5	0.093 ± 0.005
Bouvante (Eu)	0.1 ± 0.6	−0.2 ± 0.4	0.9 ± 1.5	0.084 ± 0.004
Sioux County (Eu)	−0.1 ± 0.6	0.0 ± 0.4	1.1 ± 1.4	0.111 ± 0.006
Sioux County (Eu)	−0.1 ± 0.6	0.1 ± 0.4	0.4 ± 1.5	
Bereba (Eu)	−0.3 ± 0.6	0.0 ± 0.4	−0.6 ± 1.5	0.191 ± 0.010
Pasamonte (Eu)	0.0 ± 0.6	0.0 ± 0.4	0.3 ± 1.5	0.088 ± 0.004
Serra de Mage (Eu)	−0.4 ± 0.6	−0.2 ± 0.4	0.9 ± 1.4	0.098 ± 0.007
Cachari (Eu)	−0.1 ± 0.6	−0.1 ± 0.4		0.252 ± 0.011
Cachari (Eu)	0.1 ± 0.6	0.1 ± 0.4	0.4 ± 1.4	
Cachari (Eu)	−0.2 ± 0.6	0.0 ± 0.4	0.1 ± 1.4	
Vaca Muerta (mesosiderite)	−0.1 ± 0.6	0.0 ± 0.4	0.1 ± 1.4	0.089 ± 0.002
Vaca Muerta (mesosiderite)	0.1 ± 0.6	−0.1 ± 0.4	−0.1 ± 1.4	
Moon 77215 (norite)	0.0 ± 0.6	−0.1 ± 0.4	−0.1 ± 1.4	
Moon 15475 (mare basalt)	0.1 ± 0.6	0.0 ± 0.4	−0.1 ± 1.4	
Moon 75075 (mare basalt)	−0.1 ± 0.6	−0.1 ± 0.4	0.0 ± 1.4	
Renazzo m.r. w.r. (CR2)	0.2 ± 0.6	0.0 ± 0.4	2.0 ± 1.4	0.068 ± 0.003
Renazzo m.l.	0.3 ± 0.6	0.1 ± 0.4	3.2 ± 1.5	0.073 ± 0.004
Renazzo n.m.	0.3 ± 0.6	0.1 ± 0.4	1.9 ± 1.4	0.068 ± 0.003
Renazzo n.m.	0.2 ± 0.6	0.3 ± 0.4	1.7 ± 1.5	
Allende leach 1 (HAc)	0.5 ± 0.6	0.0 ± 0.4	10.0 ± 1.5	
Allende leach 3 (HCl)	0.0 ± 0.6	−0.1 ± 0.4	2.6 ± 1.5	
Allende leach 4 (HCl/HF)	−0.1 ± 0.6	−0.1 ± 0.4	0.5 ± 1.5	
Allende leach 5 (aqua regia)	−0.3 ± 0.6	−0.1 ± 0.4	−0.1 ± 1.5	
CAI Allende USNM 4698	0.0 ± 0.6	0.0 ± 0.4	2.1 ± 1.5	0.015 ± 0.001

Table 2 (Continued).

Sample	$\epsilon^{91}\text{Zr} \pm 2\sigma_{\text{mean}}$	$\epsilon^{92}\text{Zr} \pm 2\sigma_{\text{mean}}$	$\epsilon^{96}\text{Zr} \pm 2\sigma_{\text{mean}}$	Nb/Zr $\pm 2\sigma_{\text{mean}}$
CAI Allende USNM 3529-21	$0.6 \pm 0.6$	$0.5 \pm 0.4$	$0.3 \pm 1.4$	$0.45 \pm 0.03$
CAI Allende USNM 3529-21	$0.4 \pm 0.6$	$0.2 \pm 0.4$	$1.2 \pm 1.4$	
CAI Allende USNM 3529-21	$0.6 \pm 0.6$	$0.4 \pm 0.4$	$0.4 \pm 1.7$	
CAI Allende USNM 3529-41	$0.3 \pm 0.6$	$0.1 \pm 0.4$	$2.5 \pm 1.4$	$0.05 \pm 0.002^a$
CAI Allende USNM 3529-41	$0.6 \pm 0.6$	$0.1 \pm 0.4$	$1.1 \pm 1.5$	
CAI Allende USNM 3529-41	$0.2 \pm 0.6$	$0.1 \pm 0.4$	$2.1 \pm 1.5$	
CAI Allende USNM 3529-41	$0.1 \pm 0.6$	$0.0 \pm 0.4$	$1.8 \pm 1.5$	
CAI Allende USNM 3529-44	$0.3 \pm 0.6$	$0.1 \pm 0.4$	$2.0 \pm 1.4$	$0.076 \pm 0.004$
CAI Allende USNM 3529-44	$0.5 \pm 0.6$	$0.3 \pm 0.4$	$2.3 \pm 1.5$	
CAI Allende USNM 3529-47	$-0.2 \pm 0.6$	$-0.3 \pm 0.4$	$1.3 \pm 1.5$	$0.116 \pm 0.006$
CAI Efremovka E49	$-0.1 \pm 0.6$	$0.2 \pm 0.4$	$1.3 \pm 1.5$	$0.081 \pm 0.004$

The quoted analytical uncertainties for the  $\epsilon\text{Zr}$  values reflect the external ( $2\sigma_{\text{mean}}$ ) reproducibilities including the uncertainties for the standard.

<sup>a</sup> Nb/Zr ratio from Mason and Taylor [53].

( $\epsilon^{96}\text{Zr} = 10.0 \pm 1.5$ ). Around 6% of the total Zr recovered (Table 1) was released in this leaching step. The Zr was probably hosted in alteration phases and/or metal [7,39]. In the nitric acid fraction (second step), the small Zr content of 6 ng did not permit precise isotopic analysis. Subse-

quent leaching with hot HCl yielded 21% of the total Zr. This fraction displays a small excess of <sup>96</sup>Zr. The last two leaching steps using HCl/HF and aqua regia represent chemically resistant phases and account for most of the Zr in the whole rock. Their Zr isotopic signature is identical to the terrestrial standard. A mass balance calculation of all Allende leach fractions results in  $\epsilon^{96}\text{Zr} = +1.4$  for bulk Allende. This is identical to the mean value measured for bulk Allende ( $\epsilon^{96}\text{Zr} = +1.0 \pm 1.2$ ), within uncertainty.

The Renazzo sample was separated into different fractions in order to identify carrier phases anomalous in <sup>96</sup>Zr (Table 1). The results (Fig. 2) show that all Renazzo fractions have an identical Zr isotopic pattern and display a small but significant excess of <sup>96</sup>Zr. Therefore, the carrier phase of the excess <sup>96</sup>Zr must be homogeneously distributed in the magnetic and non-magnetic phases. The same observation was made for the carrier phase of anomalous <sup>54</sup>Cr in Orgueil [39].

In addition, six CAIs separated from Allende and Efremovka were analyzed (Fig. 1b). Three of the Allende CAIs reveal a small excess of <sup>96</sup>Zr. The observed excess <sup>96</sup>Zr is not large enough to produce a well-resolved difference in the bulk Allende data presented here. However, the CAIs could be responsible for some of the excess <sup>96</sup>Zr in the Allende leachates. CAIs, for example, contain a significant amount of melilite, which can be attacked by hydrochloric acid.

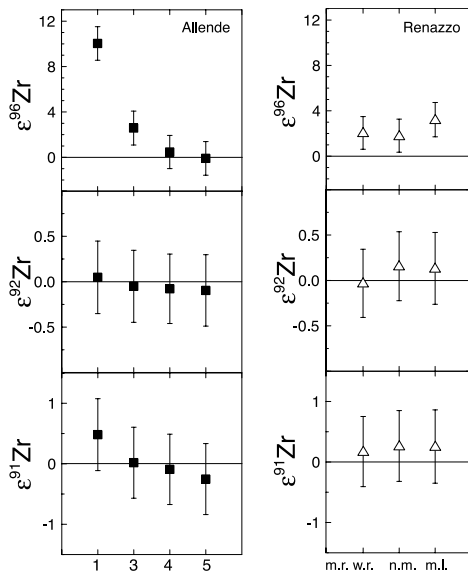


Fig. 2. Zirconium isotopic compositions for separates of Allende and Renazzo. 1 = acetic acid leachate, 3 = HCl leachate, 4 = HF/HCl leachate, 5 = aqua regia leachate, m.r. w.r. = metal-rich whole rock, n.m. = non-magnetic fraction, m.l. = magnetic leachate fraction. For details see Table 1.

## 4. Discussion

### 4.1. The bulk rock analysis

All the bulk rock data (Fig. 1a) show a remarkable homogeneity in Zr isotopic compositions. This observation contrasts with the results of previous studies on bulk rock meteorites [24,25] that identified Zr isotopic anomalies well outside the stated analytical uncertainties. It is notable that some meteorites were analyzed in both this and previous studies such as Murchison (CM2), Allende (CV3), Abee (EH4), Orgueil (CI) and Forest Vale (H4). For the first three meteorites,  $\epsilon^{96}\text{Zr}$  values up to +50 were reported [25]. The isotope  $^{96}\text{Zr}$  has a low abundance (2.8%) and two sources of isobaric interferences,  $^{96}\text{Mo}$  and  $^{96}\text{Ru}$ . The three meteorites for which  $^{96}\text{Zr}$  anomalies are cited (Allende, Murchison, Abee) are primitive meteorites, which require a Ru correction on mass 96. Unfortunately, the authors [25] provided no information about the Ru correction. They demonstrated that the Mo interference on  $^{92}\text{Zr}$  can be adequately corrected for solutions with  $\text{Mo}/\text{Zr} < 0.01$ . It is unclear, however, if this also applies to the correction on mass 96. Until these issues are resolved, it remains possible that the reported  $^{96}\text{Zr}$  anomalies are analytical artefacts that reflect insufficiently corrected interferences.

The uniformity of our bulk rock data (Fig. 1a) provides compelling evidence that the inner solar system is generally well mixed in terms of the Zr isotopic composition and this implies that the protosolar nebula was also well mixed on a planetary scale before planetesimal accretion occurred. The isotope data for other elements such as iron are in accord with this conclusion, because the observed Fe isotope variations are solely due to mass-dependent fractionation [40]. However, disk-scale isotopic heterogeneity has been proposed for e.g.  $^{26}\text{Al}$ ,  $^{41}\text{Ca}$  [41],  $^{53}\text{Mn}$  [12], O isotopes [2,10] and, most recently, Mo isotopes [16,17]. Although some of these isotopic variations might relate to processes associated with the early evolution of the sun and inner disk, the Mo isotopic variations have been interpreted in terms of a very early isotopic heterogeneity in the region of the disk that supplied the materials forming iron meteorite

and chondrite parent bodies. The magnitude of these Mo isotopic variations, particularly in iron meteorites, is a matter of debate [18,19]. However, the fact that there exist effects that vary with normalization scheme provides strong evidence of real, albeit poorly resolved heterogeneity [42].

Evidence of very large Mo and Zr isotopic heterogeneity at a very small scale is provided by presolar grains. Fig. 3 illustrates two signatures of Zr isotopes discovered in presolar grains, and similar observations exist for Mo isotopes [20,43]. If such presolar grains with different isotopic patterns were not distributed evenly within the disk, this could result in large-scale heterogeneities. Considering the concentration of Mo and Zr in Allende [44] and the average abundance and isotopic composition of these elements in SiC grains [20,23,43,45], Allende should display isotopic anomalies of the same order of magnitude for both Mo and Zr. It is at first sight puzzling, therefore, why such heterogeneities are found in Mo

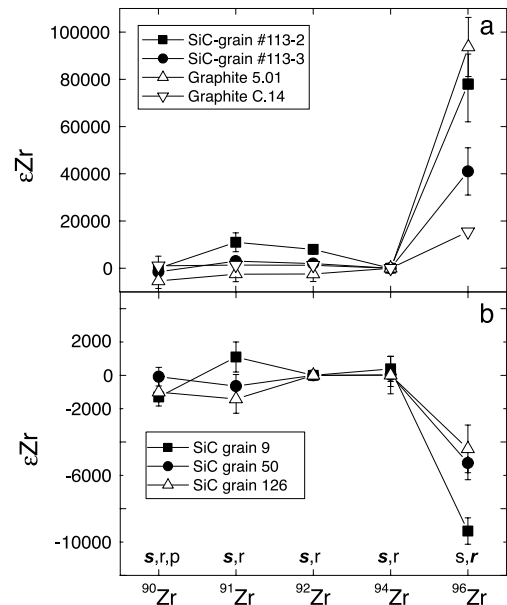


Fig. 3. (a) Zirconium isotopic patterns as a function of mass for presolar SiC grains [21] and graphite grains [20] with an *r*-process signature from the Murchison meteorite. (b) Isotopic pattern for SiC grains with an *s*-process signature [23]. For further details see references. At the bottom, the nucleosynthetic processes by which each Zr isotope can be formed are shown. Highlighted in bold is the primary nucleosynthetic process.



but not in Zr isotopic compositions. It is conceivable that such effects may exist for Zr, but that they are just below the detection limit, as the effects claimed for Mo are only a few  $\epsilon$  units. In fact the Mo anomalies reported [16,17] may be somewhat smaller than originally proposed, since later studies [18,19] have been unable to confirm the results. Assuming that the Mo anomalies are real, the data may be most simply explained by the relative proportions of *r*- versus *s*-process contributions for the single isotopes of Mo and Zr. They are greater for the isotopes of Mo than for those of Zr all of which contain mixed *r*- and *s*-process contributions.

#### 4.2. Separates of Allende and Renazzo

For the first time, Zr isotopic data of selectively dissolved fractions of carbonaceous chondrites are presented (Fig. 2). In contrast to the homogeneity of the bulk rock data, two of the Allende leachates and all separates of Renazzo display significant excess  $^{96}\text{Zr}$ . Isotopic heterogeneities measured in leach fractions of carbonaceous chondrites, therefore, not only exist for  $^{54}\text{Cr}$  [7,39],  $^{40}\text{K}$  [46] and Mo isotopes [47], but also for  $^{96}\text{Zr}$ . This provides evidence for isotopic heterogeneities at a small scale in the solar system. Small-scale heterogeneities were also discovered in presolar grains [6] and provide evidence for a solar nebula with colder regions that contain gas and distinct solid particles.

The production of  $^{96}\text{Zr}$  by cosmic ray-induced spallation or special irradiation scenarios of the early sun needs to be verified by model calculations. Nevertheless, it is unlikely that these processes are able to produce significant levels of  $^{96}\text{Zr}$  within the solar system (I. Leya, personal communication, 2003). Therefore, the excess  $^{96}\text{Zr}$  in the Allende and Renazzo fractions probably has the same nucleosynthetic origin as that in presolar grains (Fig. 3). This leads to the question whether presolar grains are the host phase of excess  $^{96}\text{Zr}$  in Allende and Renazzo. The largest excess of  $^{96}\text{Zr}$  was found for the acetic acid leachate. Although acetic acid leaching should predominantly attack phases in the matrix, where the bulk of the presolar grains is located, it is unlikely that this treat-

ment will dissolve the known varieties of presolar grains, since these are very acid-resistant. The matrix material of primitive meteorites experienced much less thermal alteration than CAIs and chondrules. Therefore, it is possible that some previously unidentified and chemically less resistant presolar grains were preserved and contributed to the excess  $^{96}\text{Zr}$  in the acetic acid leachate.

Alternatively, the excess  $^{96}\text{Zr}$  may be hosted in phases that formed within the solar system. Presolar grains that were incorporated to solar system material could have been affected by aqueous alteration thereby transferring their exotic isotopic signatures to easily leachable minerals. Furthermore, presolar grains could already have reacted with other phases or been melted or vaporized within the solar nebula, transferring there their isotopic signatures to solids formed in the solar system. The observation that three Allende CAIs preserve a significant amount of excess  $^{96}\text{Zr}$  indicates that part of the excess  $^{96}\text{Zr}$  is hosted in such a phase. CAIs are generally regarded as high-temperature condensates that formed very early in the solar system. Although extremely chemical-resistant, presolar grains are unlikely to have survived at such high temperatures. The observed  $^{96}\text{Zr}$  anomalies in CAIs, therefore, must be inherited and preserved in material that formed in the early solar system.

Comparing the present results with leaching data for other elements may help to identify the nature of the carrier phase(s). In Allende, variations of  $^{54}\text{Cr}$  [7] and  $^{96}\text{Zr}$  were observed in different leaching steps. In the present experiment, excess  $^{96}\text{Zr}$  was released by acetic and hydrochloric acids, but not by HCl/HF (Table 1, Fig. 2). In contrast, excess  $^{54}\text{Cr}$  only occurs to a limited extent in the acetic acid leachate, and is more pronounced in the HCl/HF leachate. It is important to note that the leaching procedures for Cr and Zr differ slightly. The hydrochloric acid step was only performed for Zr. Therefore, the excess  $^{54}\text{Cr}$  of the Allende HCl/HF leachate could be hosted in the same HCl-soluble carrier phase that contains excess  $^{96}\text{Zr}$ . This conclusion is supported by the results of Podosek et al. [39], who found the largest excess of  $^{54}\text{Cr}$  for Orgueil in the hydrochloric acid leachate. This indicates that ex-

cess  $^{54}\text{Cr}$  and part of the excess  $^{96}\text{Zr}$  may be hosted in similar or identical carrier phases, which have different Zr/Cr ratios. In view of nucleosynthetic models, this is viable, because most models indicate that both  $^{54}\text{Cr}$  [7] and  $^{96}\text{Zr}$  are predominantly produced in a supernova environment.

#### 4.3. Modelling

The uniformity of the bulk rock data (Fig. 1a) and the magnitude of the isotopic anomalies in presolar grains [20] can be used to estimate the magnitude of possible Zr isotope heterogeneities in the solar system. This is of more than academic interest. It is a widely held view that short-lived radionuclides like  $^{53}\text{Mn}$  could represent freshly synthesized stellar products that were injected into the protosolar nebula. The accompanying shock wave may have triggered the collapse of the protosolar nebula [48,49]. Because of the short time-scale between injection of the material and collapse of the protosolar nebula, the freshly injected material may not have had sufficient time to be completely admixed into the protosolar nebula material and this could have generated isotopic heterogeneities. The large-scale heterogeneity in  $^{53}\text{Mn}$  may be due to such a late injection of freshly produced nucleosynthetic material (e.g. [49]).

Assuming that a supernova triggered the collapse of the protosolar nebula and injected new material [48], it is possible to calculate the atom fraction of  $r$ -process Zr that can be heterogeneously distributed in the inner solar system without causing any measurable isotopic effect. This restriction is imposed by the homogeneity of Zr isotopic compositions observed for the Earth, Moon, eucrites and chondrites. The calculation was performed using the following equation:

$$\frac{{}^{96}N}{{}^{90}N} = \frac{f \times {}^{96}ab_{\text{solar}} + (1-f) \times {}^{96}ab_{\text{inj}}}{f \times {}^{90}ab_{\text{solar}} + (1-f) \times {}^{90}ab_{\text{inj}}}$$

In this equation,  ${}^iN$  represent the abundance of a specific Zr isotope with mass  $i$  in the mixture,  ${}^iab$  the abundance of a specific isotope in the solar system (solar) or in the injected material (inj) and  $f$  is the atom fraction of solar system isotopes in the mixture. The isotopic composition of the

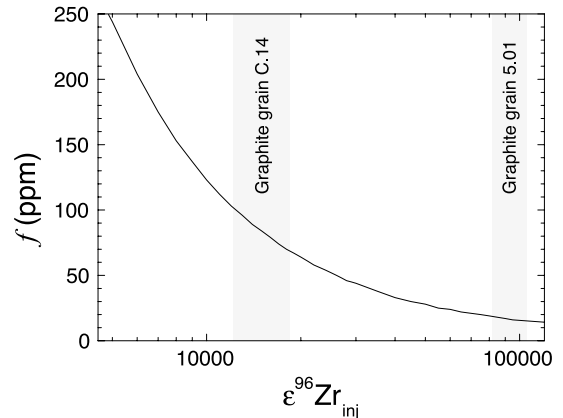


Fig. 4. The curve indicates the maximum atom fraction ( $f$ ) of Zr with distinct  $\epsilon^{96}\text{Zr}$  ( $\text{inj} = \text{injected}$ ) that can be injected into a system with  $\epsilon^{96}\text{Zr} = 0$  without producing a significant change ( $\epsilon^{96}\text{Zr} > 1.2$ ) in the Zr isotopic composition. The gray bars show the  $\epsilon^{96}\text{Zr}$  for the presolar graphite grains C.14 and 5.01 (data from [20]). The maximum atom fraction increases from 100 ppm to 130 ppm, if the exact isotopic composition of the grain C.14 is used ( $\epsilon^{90}\text{Zr}$ ,  ${}^{91}\text{Zr}$  and  $\epsilon^{92}\text{Zr} \neq 0$ ).

interstellar graphite grain C.14 (Fig. 3) was used as a lower limit of the  $r$ -process composition of the injected material. The calculation shows that the proportion of Zr derived from  $r$ -process presolar grains can only vary by less than 130 ppm for the various solar system bodies (Fig. 4). Assuming that the graphite grain 5.01 with a very high excess of  $^{96}\text{Zr}$  displays the average  $r$ -process composition, the variation is restricted to less than 15 ppm.

It is also possible that an AGB star triggered the collapse of the solar system [50]. In this case, Zr isotopes provide constraints for the differences in the proportion of Zr originating from  $s$ -process grains. Using the Zr isotopic composition of SiC grain 126 (Fig. 3), the difference has to be  $< 300$  ppm, which is somewhat higher than in the supernova scenario.

#### 4.4. The calcium–aluminum-rich inclusions

Only three of the six analyzed CAIs display a small, resolvable excess of  $^{96}\text{Zr}$  (Fig. 1b). This is consistent with previous Zr isotopic measurements for coarse-grained Allende CAIs [25,51] and the evidence for  $r$ -process signatures pre-

Table 3  
Description of the CAIs

Sample	Grain size	Group <sup>a</sup>	Excess <sup>96</sup> Zr	Reference
CAI Allende USNM 4698	Fine-grained	Group III	Yes	[52]
CAI Allende USNM 3529-21	Coarse-grained	Group V	No	[53]
CAI Allende USNM 3529-41	Coarse-grained	Group III	Yes	[53]
CAI Allende USNM 3529-44	Medium-grained	Group VI	Yes	[53]
CAI Allende USNM 3529-47	Fine-grained	Group VI	No	[53]
CAI Efremovka E49	Coarse-grained	–	No	[54]

<sup>a</sup> On the basis of rare earth element pattern.

served in FUN inclusions for samarium and neodymium [4,5]. However, there seems to be a difference between the <sup>96</sup>Zr and <sup>50</sup>Ti anomalies observed in normal CAIs. The <sup>96</sup>Zr excesses are smaller and rare compared to the ubiquitous excesses of <sup>50</sup>Ti. The occurrence of <sup>96</sup>Zr anomalies does not correlate with the petrographic type of the CAIs or with the rare earth element patterns (Table 3) [52–54]. The observation that isotopic effects are not pervasive in CAIs has also been made for the abundances of the short-lived radionuclides <sup>26</sup>Al and <sup>41</sup>Ca [55]. Diverse models have been proposed to explain this feature. Among these are the suggestions for a heterogeneous distribution of <sup>26</sup>Al in the solar nebula (e.g. [56,57]) and special irradiation scenarios including the X-wind model during the evolution of the young sun [9]. The production of <sup>96</sup>Zr within the solar system by irradiation is unlikely. A heterogeneous distribution of <sup>96</sup>Zr, however, cannot be excluded.

The existence of <sup>96</sup>Zr anomalies supports the idea that CAIs originated from material that was isotopically distinct from average solar system. The CAIs may simply have formed from too little material to sample the exact average solar system composition. The isotopic data obtained from stepwise dissolution of carbonaceous chondrites ([7,39,46,47]; this work) and the occurrence of presolar grains (e.g. [58,59]) indicates that average solar system material is built up of distinct nucleosynthetic components which can, in part, be separated. Heterogeneities at a very small scale, therefore, exist in solar system materials and could have been sampled by CAIs.

Another explanation is that CAIs formed before homogenization of the material in the protoplanetary disk was complete. As a consequence,

CAIs either sampled a heterogeneity that was already present for a longer time-scale in the protosolar nebula or the heterogeneity developed through a late injection of freshly synthesized material. Assuming a late injection, the introduced material may have been dominated by either *r*-process or *s*-process products depending on its stellar source. In the first case, the CAIs would preserve the diluted *r*-process signature of the injected material, in the latter the signature of the former average solar system composition. The latter case entails that the composition of the whole solar system was changed through the injection of predominately *s*-process material from an AGB or Wolf–Rayet star. Clearly, this scenario requires the injection of huge amounts of material, whereas the alternative model only requires that small local isotopic heterogeneities of injected *r*-process material are preserved.

However, although possible, it is not clear that the observed excess of <sup>96</sup>Zr is related to a late injection of material. In any case, some CAIs formed before mixing of solar system material was complete, such that they were able to sample a population of *r*-process-enriched material.

#### 4.5. <sup>92</sup>Nb–<sup>92</sup>Zr

Evidence for formerly live <sup>92</sup>Nb was first identified in a Nb-rich rutile from the iron meteorite Toluca [27]. An initial <sup>92</sup>Nb/<sup>93</sup>Nb of (1.6 ± 0.3) × 10<sup>−5</sup> was inferred. Three subsequent studies proposed that the initial <sup>92</sup>Nb/<sup>93</sup>Nb ratio of the solar system was in fact more than two orders of magnitude higher at ~10<sup>−3</sup> [24,28,29]. A combined Zr isotopic and U–Pb age study of an early zircon from a eucrite yielded an initial

$^{92}\text{Nb}/^{93}\text{Nb}$  of  $< 10^{-4}$  [30]. This result agrees with the most recent work, which produced the first isochrons for the Nb–Zr system and inferred a low initial value of  $< 3 \times 10^{-5}$  [31].

The Nb/Zr elemental ratio and the age of a sample determine whether the decay of the extinct radionuclide  $^{92}\text{Nb}$  would produce a measurable  $^{92}\text{Zr}$  anomaly, assuming that the solar system started with a sufficiently high  $^{92}\text{Nb}/^{93}\text{Nb}$  ratio. Hence, a high Nb/Zr ratio in an old sample should result in a large excess of  $^{92}\text{Zr}$ . Although the Nb/Zr ratios of the different bulk meteorite samples and CAIs (Table 2) vary by a factor of more than 10, no  $^{92}\text{Zr}$  anomaly is found. Since these samples are generally regarded as the oldest in the solar system, this requires a low initial  $^{92}\text{Nb}/^{93}\text{Nb}$  ratio for the solar system. Therefore, our new results are inconsistent with an initial  $^{92}\text{Nb}/^{93}\text{Nb}$  of  $\sim 10^{-3}$ .

Münker et al. [29] analyzed a bulk rock sample (60 mg) of the ordinary chondrite Adrar 003 (LL3) and found a Nb/Zr ratio of 0.166 and an  $\varepsilon^{92}\text{Zr}$  excess of  $+2.7 \pm 1.0$ . In comparison, the bulk rock samples of the eucrites Sioux County and Bereba analyzed in this work have similar Nb/Zr ratios of 0.111 and 0.191, respectively, and they display no effects in  $^{92}\text{Zr}$ . Furthermore, Münker et al. [29] presented data for a CAI which is characterized by a Nb/Zr ratio of  $\sim 0.015$  and a  $^{92}\text{Zr}$  deficit of about  $-2 \varepsilon$  units. In contrast, the Allende CAI USNM 4698 analyzed in this study also has a Nb/Zr = 0.015, but it does not display a  $^{92}\text{Zr}$  anomaly (Table 2).

These results cannot easily be explained by age differences. Sioux County and Bereba are dated by Pb isotope systematics to  $\sim 40$  Myr after the start of the solar system [60–62] and can only be reconciled with the Adrar 003 data by allowing large analytical uncertainties. However, age differences cannot account for the differences between the CAI data, because this would require that these CAIs formed over a period of more than 80 Myr, which is highly implausible [54].

The initial abundance of  $^{26}\text{Al}$  shows significant variations in CAIs [56]. This may be due to age differences or special irradiation scenarios like the X-wind model [9]. According to this model, the variations in  $^{26}\text{Al}$  originate from different irradi-

ation times of the proto-CAIs during the evolution of the early sun. Recent model calculations show that the X-winds could also produce  $^{92}\text{Nb}$  (I. Leya, personal communication, 2003). As a consequence, CAIs with variable initial abundances of  $^{92}\text{Nb}$  may be produced, if they differ in their exposure to the early solar irradiation. However, unlike  $^{26}\text{Al}$ , the high initial abundances of  $^{92}\text{Nb}$  that have been proposed are based on  $^{92}\text{Zr}$  deficits relative to average solar system [24,28,29]. This implies that the initial  $^{92}\text{Zr}/^{90}\text{Zr}$  ratio of the entire solar system was more than 2  $\varepsilon$  units lower than the present-day value. Significant amounts of  $^{92}\text{Nb}$  have to be produced by the X-wind scenario to enable such an evolution. It is feasible to consider a model in which the material that formed the Earth, Moon, chondrites and eucrites was enriched in  $^{92}\text{Nb}$  by being processed through the inner part of the accretion disk, while some CAIs escaped irradiation. Recently, a similar scenario was proposed by Clayton [63] for oxygen. In this case, the CAIs are depleted in  $^{17}\text{O}$  and  $^{18}\text{O}$  compared to the rest of the solar system. Irradiation by the early sun increases the  $^{18}\text{O}/^{16}\text{O}$  and  $^{17}\text{O}/^{16}\text{O}$  ratios of the remaining meteoritic and planetary material by up to several percent. However, some isotopic heterogeneity in oxygen still survives in bulk rock samples, whereas the homogeneity of the  $^{92}\text{Zr}$  values (Fig. 1a) requires that both  $^{92}\text{Nb}$  and  $^{92}\text{Zr}$  were homogeneously distributed in the solar system. This entails that a very efficient mixing process must have erased any heterogeneities after the solar system material was exposed to the irradiation of the early sun. In summary, it is possible to explain the different  $^{92}\text{Nb}$  data of CAIs with the X-wind model, but this requires very special circumstances, which are rather unlikely.

The new CAI data can be used to infer an upper limit for the initial  $^{92}\text{Nb}/^{93}\text{Nb}$  of the solar system. A chondritic Nb/Zr ratio of 0.076 was deduced from the chondrite data of Table 2 and this value was applied in the following age calculation. Note that this value is slightly higher than the previously applied value of  $\sim 0.065$  [64], but in excellent agreement with a recent estimate of Weyer et al. [65]. The strongest constraint on the initial  $^{92}\text{Nb}/^{93}\text{Nb}$  is provided by CAI USNM

3529-21. Even if this CAI formed as late as 10 Myr after the start of the solar system, the initial  $^{92}\text{Nb}/^{93}\text{Nb}$  ratio has to be less than  $2.5 \times 10^{-5}$ . This is in agreement with our previous result [31]. Mason and Taylor [53], however, determined a much higher Nb/Zr ratio of 0.076 for the same CAI. This difference may reflect sample heterogeneity. If the Nb/Zr ratio is 0.076 (i.e. chondritic), the data do not constrain the initial  $^{92}\text{Nb}$  abundance in a useful way. Nevertheless, further support for a low initial  $^{92}\text{Nb}$  abundance is provided by the results for CAI USNM 3529-47 and CAI USNM 4698, which both require an initial  $^{92}\text{Nb}/^{93}\text{Nb}$  for the solar system of less than  $2 \times 10^{-4}$ .

## 5. Conclusions

New Zr isotopic data show that chondrites and eucrites as well as the Moon and the Earth have identical Zr isotopic compositions despite compositions that must represent a mixture of *r*- and *s*-process components. Homogeneity in Zr isotopes thus extends over a broad range of heliocentric distance. The data, therefore, provide powerful evidence that the solar nebula was well mixed at a large scale and that presolar grains were present in nearly identical proportions through the investigated region of the disk. The presence of *r*-process components can be partly resolved by stepwise dissolution of carbonaceous chondrites as shown for Allende. The carrier phase is not yet identified. Some CAIs in Allende also display a small but distinct *r*-process signature.

Moreover, the Nb/Zr ratios and the Zr isotopic data acquired for some CAIs require an initial  $^{92}\text{Nb}/^{93}\text{Nb}$  ratio of  $< 2 \times 10^{-4}$ . All of the presented data are consistent with a low initial  $^{92}\text{Nb}/^{93}\text{Nb}$  ratio of  $< 3 \times 10^{-5}$  [27,31].

## Acknowledgements

We thank the Swiss National Science Foundation and ETH for support of this research, Y. Amelin for providing the Efremovka CAI; G.L. MacPherson and M. Linstrom for access to their meteorite collections at the Smithsonian Institu-

tion of Washington and NASA. Furthermore, we are grateful to G.W. Lugmair, R.W. Carlson and C. Münker for their helpful comments. [BW]

## References

- [1] J.H. Reynolds, Isotopic abundance anomalies in the solar system, *Annu. Rev. Nucl. Sci.* 17 (1969) 253–316.
- [2] R.N. Clayton, L. Grossman, T.K. Mayeda, A component of primitive nuclear composition in carbonaceous meteorites, *Science* 182 (1973) 485–488.
- [3] S. Niemeyer, G.W. Lugmair, Ubiquitous isotopic anomalies in Ti from normal Allende inclusions, *Earth Planet. Sci. Lett.* 53 (1981) 211–225.
- [4] G.W. Lugmair, K. Marti, N.B. Scheinin, Incomplete mixing of products from *r*-, *p*-, and *s*-process nucleosynthesis: Sm-Nd systematics in Allende inclusions, *Lunar Planet. Sci.* 9 (1978) 672–674.
- [5] M.T. McCulloch, G.J. Wasserburg, Barium and neodymium isotopic anomalies in the Allende meteorite, *Astrophys. J.* 220 (1978) L15–L19.
- [6] R.S. Lewis, T. Ming, J.F. Wacker, E. Anders, E. Steel, Interstellar diamonds in meteorites, *Nature* 326 (1987) 160–162.
- [7] M. Rotaru, J.L. Birck, C.J. Allègre, Clues to early solar system history from chromium isotopes in carbonaceous chondrites, *Nature* 358 (1992) 465–470.
- [8] S.J. Weidenschilling, Aerodynamics of solid bodies in the solar nebula, *Mon. Not. R. Astron. Soc.* 180 (1977) 57–70.
- [9] F.H. Shu, H. Shang, A.E. Glassgold, T. Lee, X-rays and fluctuating X-winds from protostars, *Science* 277 (1997) 1475–1479.
- [10] R.N. Clayton, Oxygen isotopes in meteorites, *Annu. Rev. Earth Planet. Sci.* 21 (1993) 115–149.
- [11] M.H. Thiemens, J.E. Heidenreich III, The mass-independent fractionation of oxygen: a novel isotope effect and its possible cosmochemical implications, *Science* 219 (1983) 1073–1074.
- [12] A. Shukolyukov, G.W. Lugmair, On the  $^{53}\text{Mn}$  heterogeneity in the early solar system, *Space Sci. Rev.* 92 (2000) 225–236.
- [13] A.N. Halliday, M. Rehkämper, D.C. Lee, W. Yi, Early evolution of the Earth and Moon: New constraints from Hf–W isotope geochemistry, *Earth Planet. Sci. Lett.* 142 (1996) 75–90.
- [14] P. Cassen, D.S. Woolum, Nebular fractionations and Mn–Cr Systematics, *Lunar Planet. Sci.* 28 (1997) 1536.
- [15] J.L. Birck, M. Rotaru, C.J. Allègre,  $^{53}\text{Mn}$ – $^{53}\text{Cr}$  evolution of the early solar system, *Geochim. Cosmochim. Acta* 63 (1999) 4111–4117.
- [16] Q.Z. Yin, S.B. Jacobsen, K. Yamashita, Diverse supernova sources of pre-solar material inferred from molybdenum isotopes in meteorites, *Nature* 415 (2002) 881–883.

- [17] N. Dauphas, B. Marty, L. Reisberg, Molybdenum evidence for inherited planetary scale isotope heterogeneity of the protosolar nebula, *Astrophys. J.* 565 (2002) 640–644.
- [18] D.C. Lee, A.N. Halliday, Molybdenum isotopic anomalies in the accretion disk?, *Meteorit. Planet. Sci.* 36 (2002) A85.
- [19] H. Becker, R.J. Walker, Efficient mixing of the solar nebula from uniform Mo isotopic compositions of meteorites, *Nature* 425 (2003) 152–155.
- [20] G.K. Nicolussi, M.J. Pellin, R.S. Lewis, A.M. Davis, R.N. Clayton, S. Amari, Zirconium and molybdenum in individual circumstellar graphite grains: New isotopic data on the nucleosynthesis of heavy elements, *Astrophys. J.* 504 (1998) 492–499.
- [21] A.M. Davis, M.J. Pellin, R.S. Lewis, S. Amari, R.N. Clayton, Molybdenum and zirconium isotopic composition of supernova grains, *Meteorit. Planet. Sci.* 34 (1999) A30–31.
- [22] G. Wallerstein, I. Iben Jr., P. Parker, A.M. Boesgaard, G.M. Hale, A.E. Champagne, C.A. Barnes, F. Käppeler, V.V. Smith, R.D. Hoffman, F.X. Timmes, C. Sneden, R.N. Boyd, B.S. Meyer, D.L. Lambert, Synthesis of the elements in stars: Forty years of progress, *Rev. Mod. Phys.* 69 (1997) 995–1084.
- [23] G.K. Nicolussi, A.M. Davis, M.J. Pellin, R.S. Lewis, R.N. Clayton, S. Amari, S-process zirconium in presolar silicon carbide grains, *Science* 277 (1997) 1281–1283.
- [24] C. Sanloup, J. Blichert-Toft, P. Télouk, P. Gillet, F. Albarède, Zr isotope anomalies in chondrites and the presence of  $^{92}\text{Nb}$  in the early solar system, *Earth Planet. Sci. Lett.* 184 (2000) 75–81.
- [25] Q.Z. Yin, S.B. Jacobsen, J. Blichert-Toft, P. Télouk, F. Albarède, Nb-Zr and Hf-W isotope systematics: Applications to early solar system chronology and planetary differentiation, *Lunar Planet. Sci.* 32 (2001) 2128.
- [26] D.R. Nethaway, A.L. Prindle, R.A. Van Konynenburg, Half-life of  $^{92}\text{Nb}$ , *Phys. Rev. C* 17 (1978) 1409–1413.
- [27] C.L. Harper Jr., Evidence for  $^{92}\text{Nb}$  in the early solar system and evaluation of a new *p*-process cosmochronometer from  $^{92}\text{Nb}/^{92}\text{Mo}$ , *Astrophys. J.* 466 (1996) 437–456.
- [28] Q.Z. Yin, S.B. Jacobsen, W.F. McDonough, I. Horn, M.I. Petaev, J. Zipfel, Supernova sources and the  $^{92}\text{Nb}$ - $^{92}\text{Zr}$  *p*-process chronometer, *Astrophys. J.* 535 (2000) L49–L53.
- [29] C. Münker, S. Weyer, K. Mezger, M. Rehkämper, F. Wombacher, A. Bischoff,  $^{92}\text{Nb}$ - $^{92}\text{Zr}$  and the early differentiation history of planetary bodies, *Science* 289 (2000) 1538–1542.
- [30] T. Hirata, Determinations of Zr isotopic composition and U-Pb ages for terrestrial and extraterrestrial Zr-bearing minerals using laser ablation-inductively coupled plasma mass spectrometry: Implications for Nb-Zr isotopic systematics, *Chem. Geol.* 176 (2001) 323–342.
- [31] M. Schönbächler, M. Rehkämper, A.N. Halliday, D.-C. Lee, M. Bourrot-Denise, B. Zanda, B. Hattendorf, D. Günther, Niobium-zirconium chronometry and early solar system development, *Science* 295 (2002) 1705–1708.
- [32] V.J.M. Salters, S.R. Hart, The mantle sources of ocean ridges, islands and arcs: The Hf-isotope connection, *Earth Planet. Sci. Lett.* 104 (1991) 364–380.
- [33] K.M. Barovich, B.L. Beard, J.B. Cappel, C.M. Johnson, T.K. Kyser, B.E. Morgan, A chemical method for hafnium separation from high-Ti whole-rock and zircon samples, *Chem. Geol.* 121 (1995) 1–4.
- [34] M. Schönbächler, M. Rehkämper, D.C. Lee, A.N. Halliday, Ion exchange chromatography and high precision isotopic measurements of zirconium by MC-ICPMS, *Analyst* (2003) in press.
- [35] M.A. Fehr, M. Rehkämper, M. Schönbächler, A.N. Halliday, A search for nucleosynthetic Te isotopes anomalies in carbonaceous chondrites, *Meteorit. Planet. Sci.* 38 Suppl. (2003) A135.
- [36] P. De Bièvre, M. Gallet, N.E. Holden, I.L. Barnes, Isotopic abundances and atomic weights of the elements, *J. Phys. Chem. Ref. Data* (1984) 809–891.
- [37] M. Rehkämper, M. Schönbächler, C.H. Stirling, Multiple collector ICP-MS: Introduction to instrumentation, measurement technique and analytical capabilities, *Geostand. Newsl.* 25 (2001) 23–40.
- [38] B. Hattendorf, D. Günther, M. Schönbächler, A.N. Halliday, Simultaneous ultratrace determination of Zr and Nb in chromium matrixes with ICP-dynamic reaction cell MS, *Anal. Chem.* 73 (2001) 5494–5498.
- [39] F.A. Podosek, U. Ott, J.C. Brannon, C.R. Neal, T.J. Bernatowicz, P. Swan, S.E. Mahan, Thoroughly anomalous chromium in Orgueil, *Meteorit. Planet. Sci.* 32 (1997) 617–627.
- [40] X.K. Zhu, Y. Guo, R.K. O’Nions, E.D. Young, R.D. Ash, Isotopic homogeneity of iron in the early solar nebula, *Nature* 412 (2001) 311–313.
- [41] T. Lee, F.H. Shu, H. Shang, A.E. Glassgold, K.E. Rehm, Protostellar cosmic rays and extinct radioactivities in meteorites, *Astrophys. J.* 506 (1998) 898–912.
- [42] A.N. Halliday, Inside the cosmic blender, *Nature* 425 (2003) 137–139.
- [43] G.K. Nicolussi, M.J. Pellin, R.S. Lewis, A.M. Davis, S. Amari, R.N. Clayton, Molybdenum isotopic composition of individual presolar silicon carbide grains from the Murchison meteorite, *Geochim. Cosmochim. Acta* 62 (1998) 1093–1104.
- [44] E. Jarosewich, R.S. Clarke Jr., J.N. Barrows, The Allende meteorite reference sample, Smithsonian Institute Press, Washington DC, 1987, 49 pp.
- [45] Y. Kashiv, Z. Cai, B. Lai, S.R. Sutton, R.S. Lewis, A.M. Davis, R.N. Clayton, M.J. Pellin, Synchrotron x-ray fluorescence: A new approach for determining trace element concentrations in individual presolar SiC grains, *Lunar Planet. Sci.* 32 (2001) 2192.
- [46] F.A. Podosek, R.H. Nichols Jr., J.C. Brannon, B.S. Meyer, U. Ott, C.L. Jennings, N. Luo, Potassium, stardust, and the last supernova, *Geochim. Cosmochim. Acta* 63 (1999) 2351–2362.

- [47] N. Dauphas, B. Marty, L. Reisberg, Molybdenum nucleosynthetic dichotomy revealed in primitive meteorites, *Astrophys. J.* 569 (2002) L139–L142.
- [48] A.G.W. Cameron, J.W. Truran, The supernova trigger for formation of the solar system, *Icarus* 30 (1977) 447–461.
- [49] R.H.J. Nichols, F.A. Podosek, B. Meyer, S.C.L. Jennings, Collateral consequences of the inhomogeneous distribution of short-lived radionuclides in the solar nebula, *Meteorit. Planet. Sci.* 34 (1999) 869–884.
- [50] G.J. Wasserburg, M. Busso, R. Gallino, C.M. Raiteri, Asymptotic giant branch stars as a source of short-lived radioactive nuclei in the solar nebula, *Astrophys. J.* 424 (1994) 412–428.
- [51] C.L. Harper, H. Wiesmann, L.E. Nyquist, D. Hartmann, B. Meyer, W.M. Howard, Interpretation of the  $^{50}\text{Ti}$ - $^{50}\text{Zr}$  anomaly correlation in CAI: NNSE Zr production limits and S/R/P decomposition of the bulk solar system zirconium abundances, *Lunar Planet. Sci.* 22 (1991) 517–518.
- [52] B. Mason, P.M. Martin, Geochemical differences among components of the Allende meteorite, *Smithsonian Contrib. Earth Sci.* 19 (1977) 84–95.
- [53] B. Mason, S.R. Taylor, Inclusions in the Allende Meteorite, *Smithsonian Contrib. Earth Sci.* 25 (1982) 1–30.
- [54] Y. Amelin, A.N. Krot, I.D. Hutcheon, A.A. Ulyanov, Lead isotopic ages of chondrules and calcium-aluminum-rich inclusions, *Science* 297 (2002) 1678–1683.
- [55] S. Sahijpal, J.N. Goswami, Refractory phases in primitive meteorites devoid of  $^{26}\text{Al}$  and  $^{26}\text{Ca}$ : Representative samples of first solar system solids?, *Astrophys. J.* 509 (1998) L137–40.
- [56] G.J. MacPherson, A.M. Davis, E.K. Zinner, The distribution of aluminum-26 in the early solar system – a reappraisal, *Meteoritics* 30 (1995) 365–386.
- [57] J.A. Wood, Meteoritic evidence for the infall of large interstellar dust aggregates during the formation of the solar system, *Astrophys. J.* 503 (1998) L101–104.
- [58] E. Anders, E. Zinner, Interstellar grains in primitive meteorites: Diamond, silicon carbide, and graphite, *Meteoritics* 28 (1993) 490–514.
- [59] G.R. Huss, R.S. Lewis, Presolar diamond, SiC, and graphite in primitive chondrites: Abundances as a function of meteorite class and petrologic type, *Geochim. Cosmochim. Acta* 59 (1995) 115–160.
- [60] M. Tatsumoto, R.J. Knight, C.J. Allègre, Time differences in the formation of meteorites as determined from the ratio of lead-207 to lead-206, *Science* 180 (1973) 1279–1283.
- [61] R.W. Carlson, F. Tera, N.Z. Boctor, Radiometric geochronology of the eucrites Nuevo Ladreo and Béréba, *Lunar Planet. Sci.* 19 (1988) 166–167.
- [62] F. Tera, R.W. Carlson, N.Z. Boctor, Radiometric ages of basaltic achondrites and their relation to the early history of the solar system, *Geochim. Cosmochim. Acta* 61 (1997) 1713–1731.
- [63] R.N. Clayton, Self-shielding in the solar nebula, *Nature* 415 (2002) 860–861.
- [64] K.P. Jochum, A.J. Stolz, G. McOrist, Niobium and tantalum in carbonaceous chondrites: Constraints on the solar system and primitive mantle niobium/tantalum, zirconium/niobium, and niobium/uranium ratios, *Meteorit. Planet. Sci.* 35 (2000) 229–235.
- [65] S. Weyer, C. Münker, M. Rehkämper, K. Mezger, Determination of ultra-low Nb, Ta, Zr and Hf concentrations and the chondritic Zr/Hf and Nb/Ta ratio by isotope dilution analyses with multiple collector ICP-MS, *Chem. Geol.* 187 (2002) 295–313.